Spectrochimica Acta Part A: Molecular and Biomolecular Spectroscopy 214 (2019) 451–458

Contents lists available at ScienceDirect

Spectrochimica Acta Part A: Molecular and Biomolecular Spectroscopy

journal homepage: www.elsevier.com/locate/saa

Specific fluorometric assay for direct determination of amikacin by molecularly imprinting polymer on high fluorescent g-C_3N_4 quantum dots

Javad Hassanzadeh [a], Babak Rezaei Moghadam [b,c], Ali Sobhani-Nasab [d,e], Farhad Ahmadi [f,g], Mehdi Rahimi-Nasrabadi [b,c,*]

[a] Research Laboratory of Advanced Water and Wastewater Treatment Processes, Department of Applied Chemistry, Faculty of Chemistry, University of Tabriz, 51666-16471 Tabriz, Iran
[b] Nanobiotechnology Research Center, Baqiyatallah University of Medical Sciences, Tehran, Iran
[c] Faculty of Pharmacy, Baqiyatallah University of Medical Sciences, Tehran, Iran
[d] Social Determinants of Health (SDH) Research Center, Kashan University of Medical Sciences, Kashan, Iran
[e] Core Research Lab, Kashan University of Medical Sciences, Kashan, Iran
[f] Physiology Research Center, Iran University of Medical Sciences, Tehran, Iran
[g] Department of Medicinal Chemistry, School of Pharmacy-International Campus, Iran University of Medical Sciences, Tehran, Iran

ARTICLE INFO

Article history:
Received 22 October 2018
Received in revised form 6 January 2019
Accepted 17 February 2019
Available online 19 February 2019

Keywords:
Amikacin
G-C_3N_4 quantum dots
Molecularly imprinting polymer
Fluorescence

ABSTRACT

Here, a specific and reliable fluorometric method for the rapid determination of amikacin was developed based on the molecularly imprinting polymer (MIP) capped g-C_3N_4 quantum dots (QDs). g-C_3N_4 QDs were obtained by facile and one-spot ethanol-thermal treatment of bulk g-C_3N_4 powder and showed a high yield fluorescence emission under UV irradiation. The MIP layer was also created on the surface on QDs, via usual self-assembly process of 3-aminopropyl triethoxysilane (APTES) functional monomers and tetraethyl ortho-silicate (TEOS) cross linker in the presence of amikacin as template molecules. The synthesized MIP-QDs composite showed an improved tendency toward the amikacin molecules. In this state, amikacin molecules located adjacent to the g-C_3N_4 QDs caused a remarkable quenching effect on the fluorescence emission intensity of QDs. This effect has a linear relationship with amikacin concentration and so, formed the basis of a selective assay to recognize amikacin. Under optimized experimental conditions, a linear calibration graph was obtained as the quenched emission and amikacin concentration, in the range of 3–400 ng mL^{-1} (4.4–585.1 nM) with a detection limit of 1.2 ng mL^{-1} (1.8 nM). The high selectivity of MIP sites as well as individual fluorescence properties of g-C_3N_4 QDs offers a high specific and sensitive monitoring method for drug detection. The method was acceptably applied for the measurement of amikacin in biological samples.

1. Introduction

Amikacin (O-3-amino-3-desoxy-a-D-glucopyranosyl-(1-6)-O-[6-amino-6-desoxy-a-d-glucoyra-nosyl-(1-4)]-N1-(4-amino-2-hydro-xy-1-oxobutyl)-2-desoxy-d-streptamine, $C_{22}H_{43}N_5O_{13}$) sulfate is a semi-synthetic and water soluble antibiotic (Fig. 1) related to the aminoglycosides [1]. In comparison to other aminoglycosides, amikacin has fewer sites susceptible to enzymatic attacks, and therefore, it can suppress drug resistance to some similar antibiotics, such as kanamycin, gentamicin and tobramycin [2]. On the other hand, unsuitable usage of amikacin by patients can cause perilous side effects like ototoxicity and nephrotoxicity. For example, the beneficial dose of amikacin is usually 15 mg/kg of body weight, which can be harmfulness for preterm infants with premature renal actions [3]. Consequently, monitoring and determination of amikacin concentration in biological media have a great important for the therapeutic studies or toxic control. For this aim, a reliable, sensitive and specific method is vital for the trace analysis of amikacin sulfate. The most of determination methods reported for amikacin sulfate are based on chromatographic techniques [4–6], capillary electrophoresis [7], spectrophotometry [8], luminescence methods [3,9] and electrochemical methods [10]. These methods encounter some problems, such as need for special derivatization or pretreatment process, special instruments, low sensitivity and selectivity.

In recent years, the use of nanostructures in diverse technological application like photocatalyst, supercapacitor, energy storage and etc. has grown to a great extent [11–19]. In this regard using nanostructures in modified sensors and electrochemical sensors is a field of interest [20–25]. Development of a simple, reliable and specific method for the

* Corresponding author at: Nanobiotechnology Research Center, Baqiyatallah University of Medical Sciences, Tehran, Iran.
E-mail address: rahimi@bmsu.ac.ir (M. Rahimi-Nasrabadi).

https://doi.org/10.1016/j.saa.2019.02.067
1386-1425/

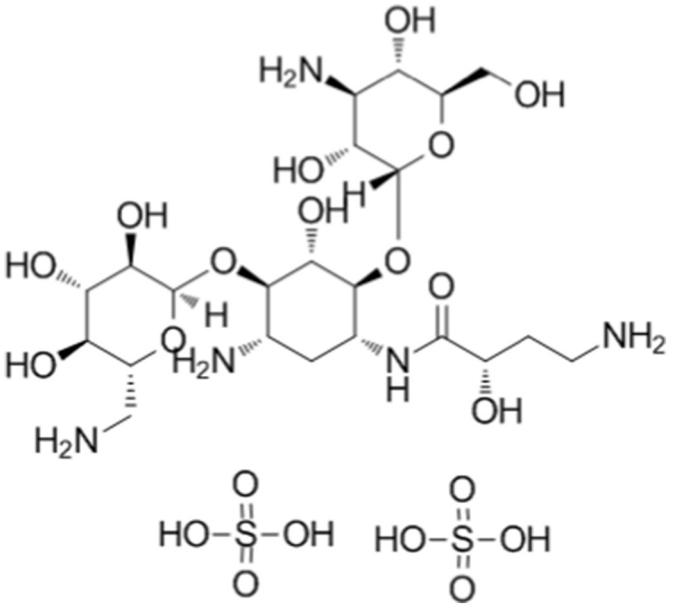

Fig. 1. Chemical structure of amikacin.

determination of amikacin in real samples is the main aim of the present research. High sensitive and low-cost fluorometric methods can be beneficial for this aim. In this regards, high luminescent quantum dots (QDs) have been extensively applied in sensing area, because of their distinctive photo-stability, wide absorption area, great quantum efficiency and the narrow emission band with large Stokes shift [26,27]. Carbon-based quantum dots with their exceptional optical behavior are mostly preferred and used as promising alternatives to organic dyes or traditional QDs [28,29]. They can overcome to the most of limitation, like serious toxicity of heavy metals in the semiconductors QDs or the inferior photo-bleaching of organic dyes [28,30,31]. Currently, graphitic carbon nitride (g-C_3N_4) with an analog layered structure to graphene, has been considered in literature [32,33]. It consist of C—N layers with weak van der Waals between them, which facilitate its exfoliation into zero dimensional QDs by external forces [34]. Furthermore, the sp^2 C—N band in a conjugated tri-s-triazine structure and the suitable band gap (around 2.7 eV) [35] provide an intensive blue fluorescence [36]. g-C_3N_4 QDs have strong quantum confinement and edge effects and show outstanding spectral features. Therefore, they have been extensively applied in optical sensing or bio-imaging [32,35,36].

On the other hand, molecular imprinting is known as an effective process to produce simulated recipient sites with a high affinity to interested molecules [37,38]. The process includes the polymerization of functional monomers in the presence of interested molecules as template. Another monomer is also used to create a high degree of crosslinking leading to the solid matrix [39]. The produced molecular imprinted polymers (MIPs) have a great specificity and high stability [38]. They have interesting applications in various areas such as sensor designing, extraction and artificial enzymes [40–43]. The link between the specific reception of MIPs and the sensitive fluorescence detection systems based on g-C_3N_4 QDs can be an appealing field in the selective and sensitive recognition of important analytes [44,45].

To the best of our knowledge, there is not any application of MIPs-capped g-C_3N_4 QDs for the detection of amikacin. In present work, a high sensitive and selective method for the simple and cost-effective detection of amikacin in biological samples have been introduced based on fluorescent MIP-coated g-C_3N_4 QDs. The applied QDs were prepared by one-spot ethanol-thermal treatment of bulk g-C_3N_4 powder. Then, a MIP layer was formed on the surface of QDs, via self-assembly reaction of 3-aminopropyl triethoxysilane (APTES) functional monomers and tetraethyl ortho-silicate (TEOS) cross linker in the presence of amikacin as template molecules. The synthesized MIP/g-C_3N_4 QDs composite has an intensive fluorescence emission which can be altered by addition of amikacin. Also, an improved selectivity toward the amikacin molecules was obtained by MIP technique. Amikacin molecules can be selectively adsorbed into the MIP sites and placed nearby the QDs, affecting their fluorescence emission intensity. The decrease in the detected fluorescence signal was proportional to amikacin concentration. Accordingly, a selective method was provided to the accurate recognition of amikacin. The method is more cost-effective and simple with a high sensitivity to amikacin. A schematic image for the offered system was provided in Fig. 2.

2. Experimental section

2.1. Chemicals and apparatus

Tetraethyl orthosilicate (TEOS), 3-aminopropyl triethoxysilane (APTES), melamine, ethanol and KOH were purchased from Sigma Aldrich (www.sigmaaldrich.com). Stoke solution of amikacin sulfate was prepared by dissolving its pure powder (Exir pharmaceutical Co., Tehran, Iran) in deionized water.

Fluorometric analysis were performed using a Shimadzu spectrofluorometer (RF-5301 PC, www.shimadzu.com). UV–visible absorption spectra were obtained by means of a Shimadzu spectrophotometer (UV-1800). Also, the morphology and chemical structure of synthesized g-C_3N_4 QDs were studied by transmission electron microscopy (TEM, Leo 906, Zeiss, Germany), emission scanning electron microscopy (Mira3 FEG SEM, Czech Republic), Fourier transform infrared spectrometry (FTIR, Tensor 27, Bruker, Germany) and X-ray diffraction (XRD) method (D5000, Siemens, Germany; by a Cu Kα exciting source and λ = 1.54056 Å).

2.2. Synthesis of g-C_3N_4 quantum dots

The synthesis of g-C_3N_4 quantum dots (QDs) was performed by ethanol-thermal pretreatment of bulk g-C_3N_4 powder as precursor [32]. First, melamine powder (6 g) was heated at 650 °C for a 2.5 h time period. The heating process was performed in an open alumina crucible (The ramp rates for heating and cooling processes were 3 °C/min). The bulk g-C_3N_4 powder (~2 g) was obtained by grounding the initial product using an agate mortar. Then, in order to synthesize g-C_3N_4 QDs, a dispersion of bulk powder in ethanol (30 mg/30 mL) was prepared and mixed with KOH concentrated solution (0.45 mL). The mixture was stirred for at least 15 min and then heated for 16 h in a Teflon-sealed autoclave (180 °C). The resulted suspension was cooled and then vacuum-filtrated by means of a 0.22 μm cellulose ester membrane to separate the agglomerated or outsized particles. The excessive reagents including ethanol and KOH were also removed by dialysis (1000 Da bag) of yellowish suspension against deionized water. After a lyophilization process, the yellow g-C_3N_4 QDs were obtained. The g-C_3N_4 QDs were redispersed in water for our examinations.

The quantum yield of synthesized fluorescent g-C_3N_4 QDs was calculated using quinine sulfate as a reference material (quantum yield = 0.56 in 0.1 M H_2SO_4) [32].

2.3. Preparation of MIP-coated g-C_3N_4 quantum dots

The MIP layer was created on the surface of g-C_3N_4 QDs by co-polymerization reaction of TEOS (as cross-linker) and APTES (as main monomer) monomers. In brief, the mixture of APTES (500 μL) and amikacin (20 mL ethanol solution containing 100 mg amikacin as template) was agitated for 15 min. 2 mL TEOS and then 500 mg g-C_3N_4 QDs were added, respectively. The mixture was stirred for another 5 min and 2 mL NH_3 solution (8% in H_2O) was added. Finally, the solution was sealed and stirred for a 16 h time period. On the other hand, non-imprinted polymer (NIP)-capped g-C_3N_4 QDs were also prepared by a

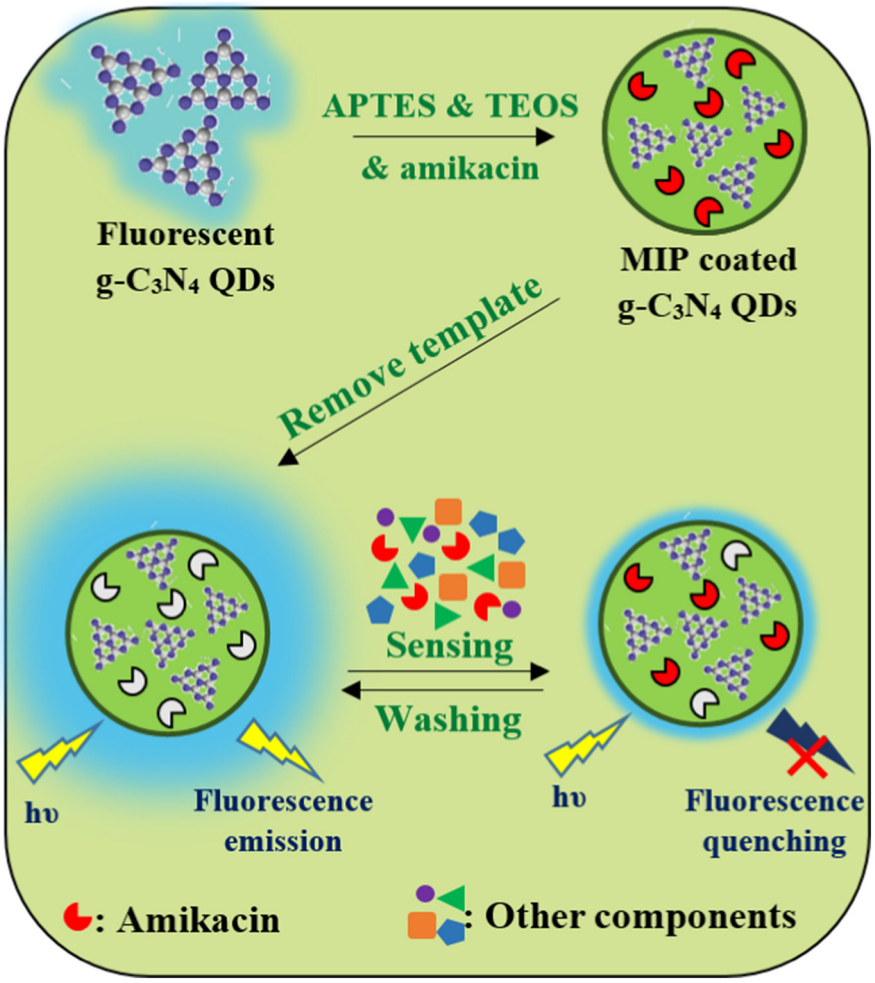

Fig. 2. Schematic design for the fluorometric detection of amikacin by MIP coated g-C_3N_4 QDs.

same procedure, but without template molecules. The produced MIP/NIP-modified *g-C_3N_4* QDs were collected by their centrifugation. They were washed with ethanol for at least three times to evacuate the template sites. The washing process for MIP-modified QDs should be resulted in their FL emission intensity approximately identical with NIP-modified QDs.

2.4. Fluorescence experiments

The fluorometric determination of amikacin was accomplished in batch state. Constant amounts (250 μL, 150 mg L^{-1}) of synthesized MIP-modified QDs were mixed with standard amikacin solutions (with different concentrations) or its sample solution. Tris buffer (500 μL, 0.02 M) was added to adjust the pH of solutions to 7. The mixtures were effectually mixed and their final volumes was reached to 5 mL using deionized water. After 5 min stirring process, the fluorescence intensities were recorded at 520 nm (λ_{ex} = 374 nm) for all solutions.

2.5. Sample preparation

The applicability of developed method for real sample was assessed by some spiked water samples or human urines. Certain amounts of amikacin standard solution were added to the samples and then, they were applied for the determination of amikacin concentration by developed method after suitable dilutions. No additional pretreatment processes were needed for analyzed samples, except the elimination of their suspended particles by means of 220 nm micro-porous filters. The concentration of amikacin in real samples were obtained by standard addition method.

3. Results and discussion

As showed in Fig. 2, the MIP-capped g-C_3N_4 quantum dots were applied for the selective recognition of amikacin in aqueous samples. First, g-C_3N_4 QDs were synthesized by a recently reported method, resulting in high intensive fluorescent QDs. Then, MIP layer was created by the self-assembly process of certain monomers and cross-linkers. The amikacin was also used as template molecules to generate specific sites in polymeric matrix. The synthesis procedure was green, simple, economic and relatively rapid. To the best of our knowledge, no MIP-based fluorescent method has been reported for the detection of amikacin using g-C_3N_4 QDs.

3.1. Characterization of g-C_3N_4 QDs

TEM images for g-C_3N_4 QDs and its composite with MIP layer were shown in Fig. 3a and b, indicating the uniform and monodispersed particles with average sizes of ~5.5 and 35 nm, respectively. So, an about 30 nm polymeric MIP layer can be considered on the g-C_3N_4 QDs. The HR-TEM image for g-C_3N_4 QDs showed their highly crystalline structure with a lattice distance of ~0.21 nm (Inset of Fig. 3a). The AFM image (Fig. 3c) also showed the low thickness of the obtained g-C_3N_4 QDs (below 2 nm), so these QDs contain a single layer or a few layers of C—N sheets.

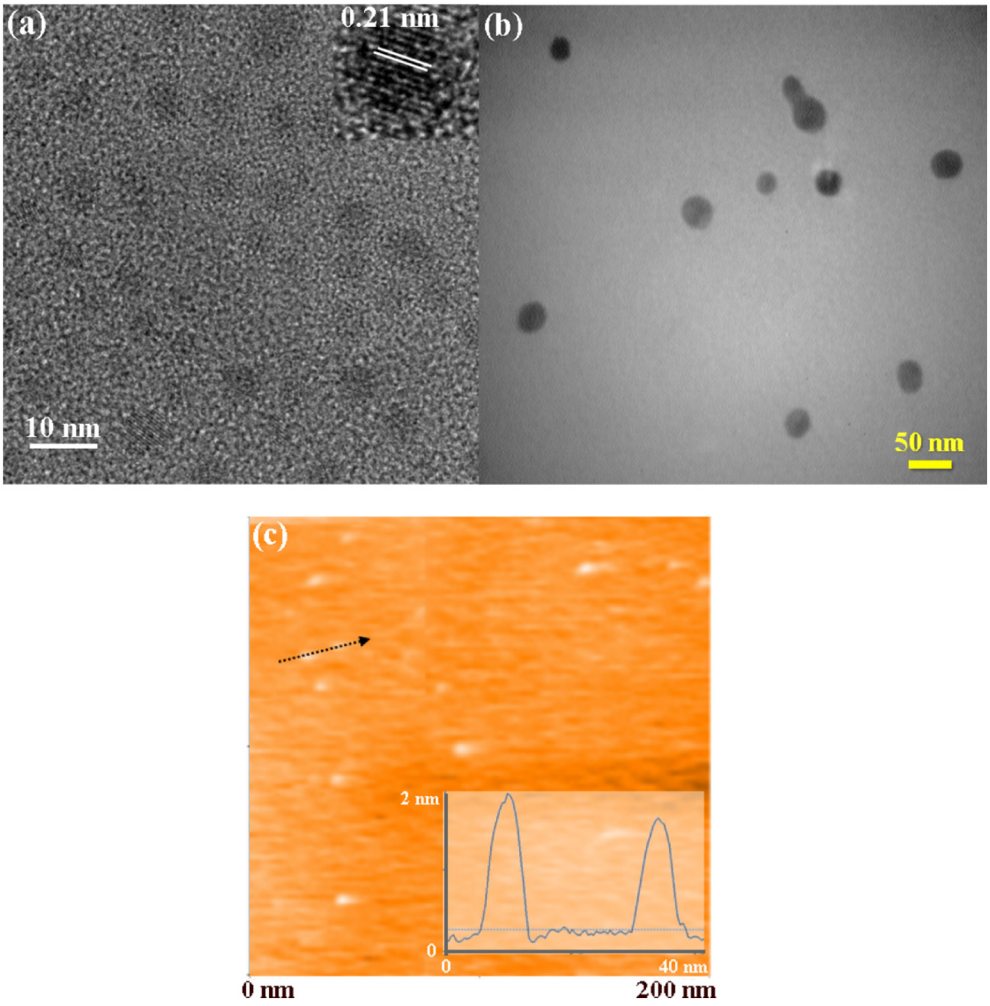

Fig. 3. TEM images for g-C_3N_4 QDs (a) and its composite with MIP layer (b); AFM image for g-C_3N_4 QDs (c).

XRD pattern was applied for the characterization of crystalline structure of produced g-C_3N_4 QDs (Fig. 4a), which indicated one broad diffraction peak at 2θ value of about 27.8°. However, two specific peaks are observed for bulk g-C_3N_4 at about 13.1° and 27.8° (Fig. 4a). The peak at 27.8° is relatively sharp showing the inter-planar stacking of C—N sheets, but the additional weak peak observed at 13.1° is associated to the aromatic structures. The fine and low-layer building of g-C_3N_4 QDs leads to the highly weakened peak at 27.8° and disappearance of 13.1° peak. This subject demonstrate the effective exfoliation process synthesis step [32].

The additional investigation for synthesized QDs was performed by FT-IR method (Fig. 4b). The main absorption bands in the spectrum of g-C_3N_4 QDs were located at around 1060 cm^{-1} (stretching C—O), 1409 cm^{-1} (stretching C—N), 1580 cm^{-1} (stretching C═N) and 1628 cm^{-1} (stretching C═O), respectively. Also, the stretching vibration of O—H/N—H bonds created a broad peak at about 3430 cm^{-1}. For MIP-capped QDs, the specific bands of Si—O bonds were appeared at 1110 and 1021 cm^{-1}. Also, the relatively strengthened N—H band was observed at 1620 cm^{-1}.

UV–vis absorption and fluorescence emission spectra were also recorded for the optical investigation of prepared g-C_3N_4 QDs. The absorption spectrum showed a weak band at about 360 nm which is related to the n-π* transition of the carbonyl and C═N bonds. On the other hand, the fluorescence spectrum of g-C_3N_4 QDs showed an excitation wavelength-dependent feature, with a maximum emission intensity at 410 nm (while the excitation wavelength is 320 nm) (Fig. 4c).The inherent emission behavior of g-C_3N_4 QDs has been connected to the sp^2 C—N bonds in conjugated tri-s-triazine assemblies. The optical selection of particles with diverse dimensions (quantum effect) and also extensive dispensing of emissive trap sites on the surface of QDs are the reason for the change in emission wavelength by changing the excitation wavelength [32].

Finally, the quantum yield and also the stability of emission intensity were studied for the g-C_3N_4 QDs and their MIP-coated form. Using quinine sulfate standard material, the quantum yields of 41% and 32% were obtained for free QDs and MIP-coated ones, respectively. The stability results illustrated a constant emission intensity of for at least 10 day for both free and MIP-coated QDs. The data were attained by 10 repeated determinations for a constant concentration of nanomaterials. The relative standard deviations (RSD) were acceptable (0.5%–1.8%).

3.2. MIP-coated g-C_3N_4 QDs for the determination of amikacin

The synthesized MIP-coated g-C_3N_4 QDs were exploited for the reliable and selective recognition of amikacin. In this structure, the MIP specific sites had been generated in the presence of amikacin as template molecules. The molecular imprinting process involved the self-assembly reaction of APTES monomers on the surface of QDs, while the TEOS was also applied as cross-linking monomers. The template molecules were entrapped into the polymeric shell throughout the polymerization process. The connection of template molecules with their surrounding media are often non-covalent, probably with amino groups of APTES. An efficient washing step can eliminate the template molecules and leave specific vacant sites matching to amikacin molecules

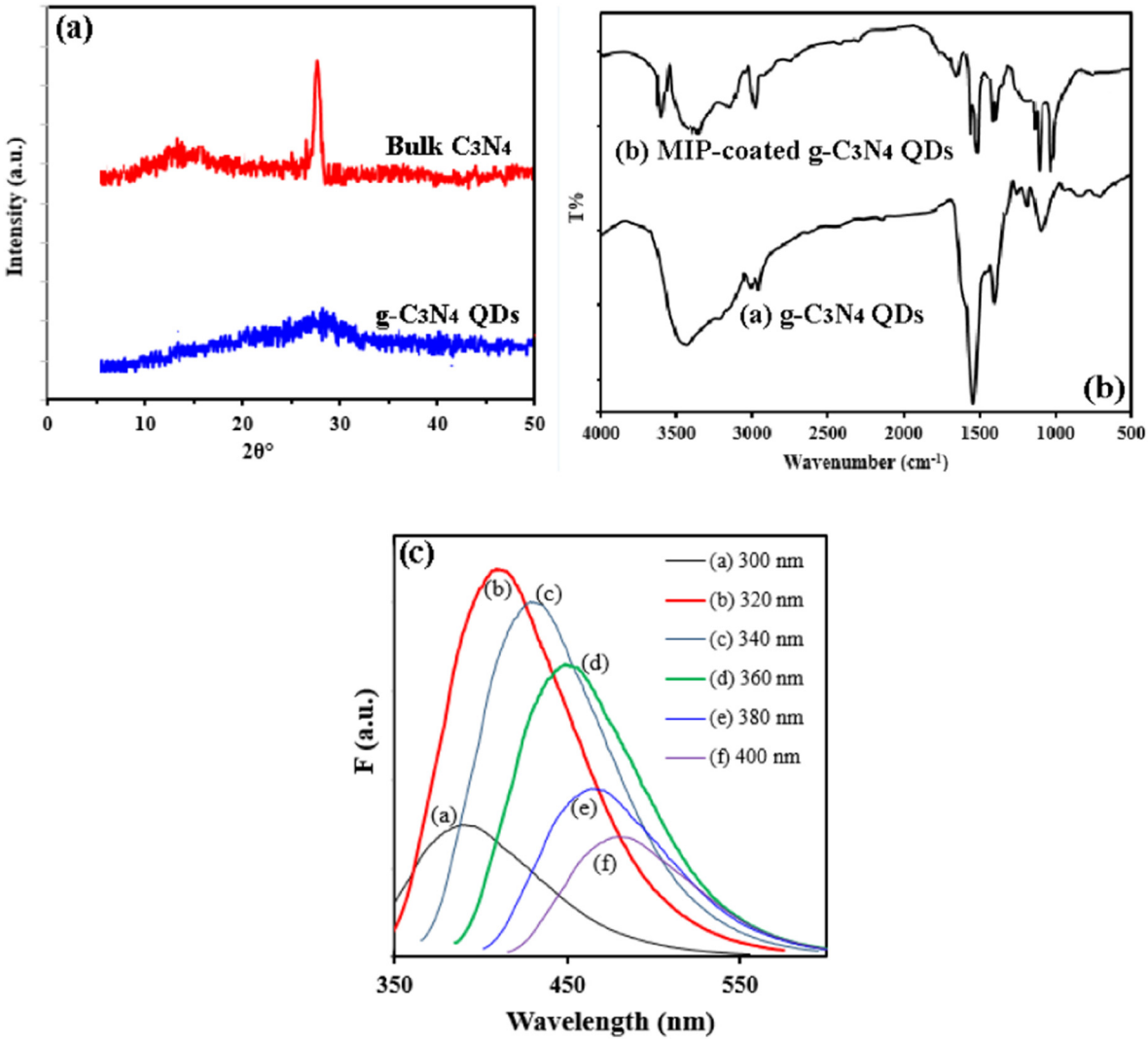

Fig. 4. a) XRD patterns for bulk g-C_3N_4 and g-C_3N_4 QDs; b) FTIR spectra for g-C_3N_4 QDs and its composite with MIP layer; (c) fluorescence spectra for g-C_3N_4 QDs with different excitation wavelengths.

in shape and functional groups. Consequently, an improved selectivity can be obtained without serious interfering effect from other similar compounds. Also, g-C_3N_4 QDs also acted as optical antenna to recognize the absorbed amikacin molecules in MIP sites. The high emission efficiency of applied QDs led to enhanced sensitivity. The presence of amikacin near the g-C_3N_4 QDs led to a quenching effect on their fluorescence intensity (Fig. 5). Initial investigations showed that the diminution effect was increased by an increasing in the amikacin concentration. So, it can be considered as a simple platform for the rapid and economic determination of amikacin.

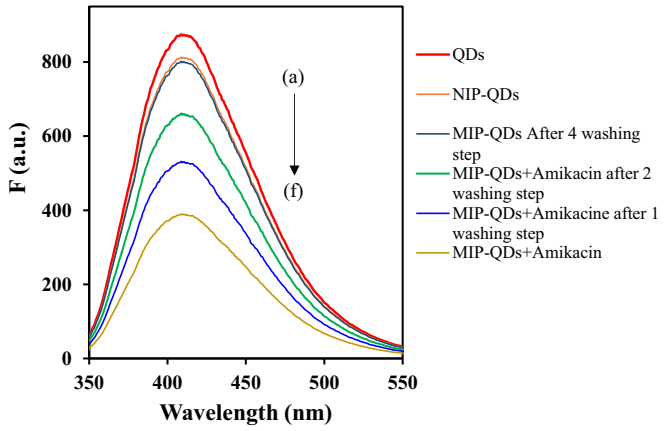

Fig. 5. Fluorescence spectra for (a) g-C_3N_4 QDs, (b) NIP-coated g-C_3N_4 QDs and (c) MIP-coated g-C_3N_4 QDs after 4 washing step, (d) MIP-coated g-C_3N_4 QDs after 2 washing step, (e) MIP-coated g-C_3N_4 QDs after 1 washing step, (f) MIP-coated g-C_3N_4 QDs.

The NIP-coated QDs were also used to further selectivity or comparison experiments. The fluorescence emission of MIP-coated g-C_3N_4 QDs ($\lambda_{em} = 410$ nm and $\lambda_{ex} = 320$ nm) displayed a remarkable quenching behavior in the presence of amikacin (template) molecules. Removing the amikacin molecules from the MIP sites using a proper washing process could restore the fluorescence intensity (Fig. 5). The washing step and thoroughly elimination of template molecules from the MIP sites on the surface of g-C_3N_4 QDs was controlled by comparing the obtained fluorescence intensity with the emission of NIP-coated QDs. Without any template, the fluorescence intensities must be equal for the NIP- and MIP-coated QDs.

3.2.1. Optimization experiments

The sensitivity of designed probe can be improved by optimization of key factors which can affect the obtained signal intensity. In this respect, the effect of pH and incubation time for adsorbing amikacin in MIP sites were examined (Fig. 6). Firstly, the pH of reaction solution was altered in the wider range of 4–12 and the fluorescence responses

($\Delta F = -F - F_0$, F_0 and F illustrate the fluorescence intensity of MIP-coated g-C_3N_4 QDs in the absence and presence of amikacin, respectively) for a constant concentration of amikacin were followed (Fig. 6a). The results showed a lower signal in acidic or high basic pHs, and a suitable sensitivity was obtained for pH range of 6–9. The proper buffer for adjusting pH was Tris, and other examined buffers (phosphate, ammonium acetate, and bicarbonate) led to a lower signal. The decreased signals in lower and higher pHs can be described by decrease in the fluorescence efficiency of applied QDs. For example, the protonation of nitrogen at low pH can deactivate the fluorescence feature of QDs [32], leading to lower emission intensities. Also, the change in the functional groups of MIP sites in different pHs can be considered as an important reason which affect the adsorbing of amikacin in these sites. This event leads to the lower responses of probe in some pHs.

For the investigation of incubation time effect on the sensitivity of developed probe, different time periods were considered for the adsorbing of amikacin in a constant concentration into the MIP-coated g-C_3N_4 QDs (Fig. 6b). The data showed a rapid decrease in the fluorescence intensity of MIP-coated g-C_3N_4 QDs after the addition of amikacin. The fluorescence intensity was reached to a constant value after 5 min and so, we considered 7 min as the optimum incubation time for subsequent experiments.

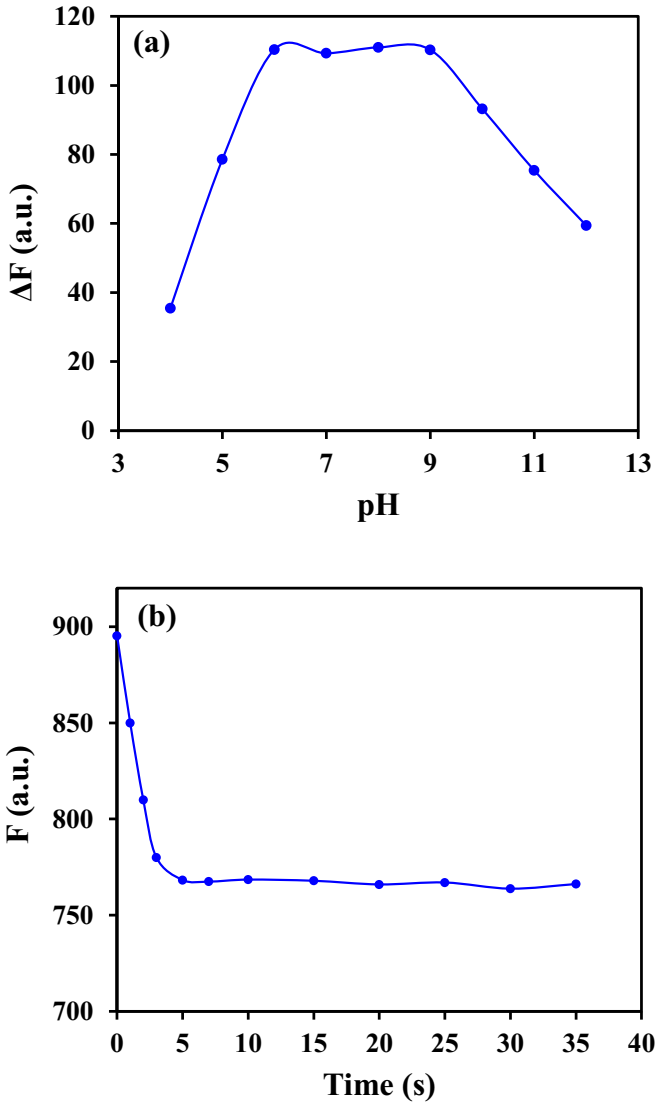

Fig. 6. Optimization of pH and incubation time in the determination process of amikacin by developed method.

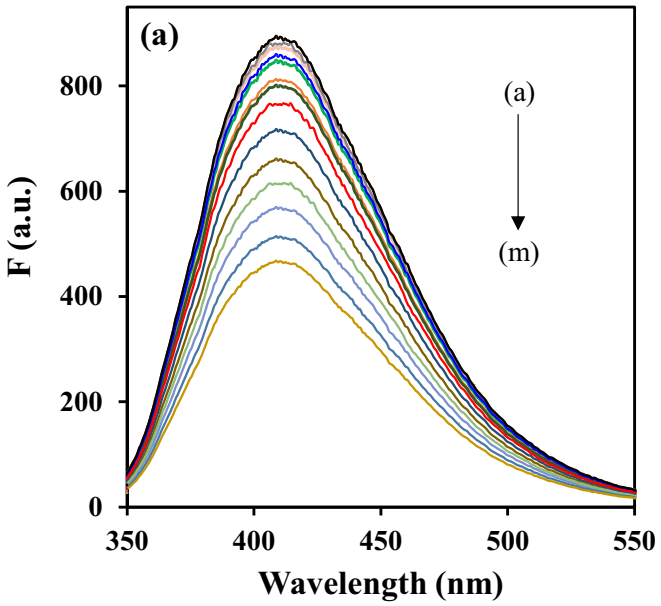

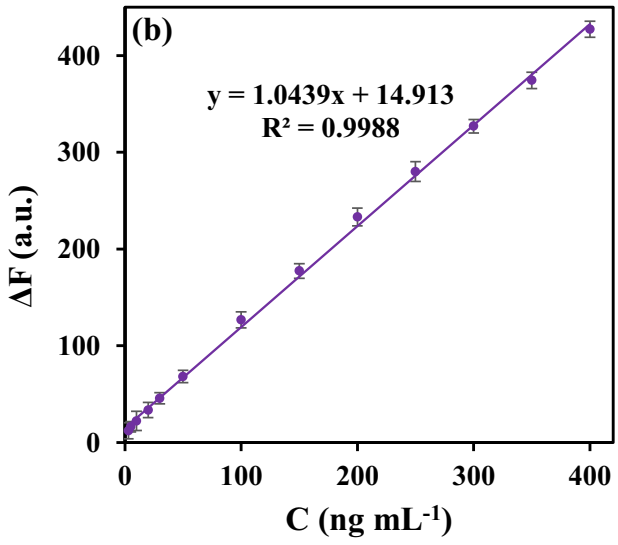

Fig. 7. a) Fluorescence spectra for MIP-coated g-C_3N_4 QDs in the presence of increasing concentrations of amikacin and, b) corresponding calibration curve.

3.2.2. Effect of amikacin concentration

The emission intensity of MIP-coated g-C_3N_4 QDs was diminished by addition of amikacin even in trace amounts (Fig. 7a). This quenching effect was proportional to the amikacin concentration and a linear

Table 1
Interfering effect of some common species on the determination of 100 ng mL^{-1} amikacin (in optimum condition).

Coexisting substance	Tolerance limit (interference to analyte ratio)
Ca^{2+}, Mg^{2+}, Na^{+}, K^{+}, CO_3^{2-}, NO_3^{-}, Cl^{-}	3200
Al^{3+}, Mn^{2+}, PO_4^{3-}, SO_4^{2-}, oxalate	2400
Fe^{3+}, Cr^{3+}, HCO_3^{-}, CH_3COO^{-}	1500
Ni^{2+}, Fe^{2+}, glucose, ascorbic acid	1350
Uric acid, citrate, glutathione	1100
Cysteine	800
I^{-}, Cu^{2+}, Zn^{2+}, Pb^{2+}, Cd^{2+}	250
Hg^{2+}	100

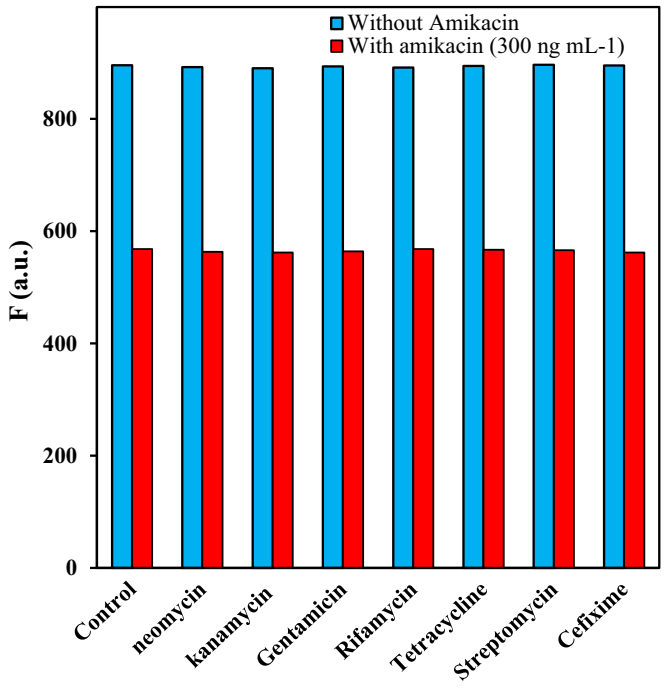

Fig. 8. Interfering effect of some similar compounds on the determination of amikacin with developed method.

calibration graph was achieved in the amikacin concentration range of 3–400 ng mL^{-1} (4.4–585.1 nM), as the fluorescence responses, ΔF, against to the amikacin concentration (C, ng mL^{-1}). The regression equation was $\Delta F = 1.0439(C) + 14.913$ ($R^2 = 0.9988$) (Fig. 7b). The limit of detection for this method was obtained 1.2 ng mL^{-1} (1.8 nM) using $3S_b/m$ (S_b is standard deviation for five replicate determination of F_0 and, m is the slope of calibration curve). RSD values were also calculated for repeated determinations of 10 and 200 ng mL^{-1} amikacin. The obtained results (3.62 and 1.93%, respectively) confirmed the proper reproducibility of the designed probe.

3.2.3. Selectivity experiments

The selectivity of developed system for the determination of amikacin was investigated by analysis of amikacin standard solution (100 ng mL^{-1}) in the presence of increasing amounts of some probable interfering species which can be exist in real samples. The analysis process was performed according to the described general procedure in Section 2.4. A relative error of <5% was considered as the tolerable interfering concentration ratios. The obtained results are showed in Table 1. No remarkable interfering effect was observed for the examined species in mentioned concentrations. On the other hand, the concentration for the most of inspected substances in considered real samples are below these levels. Therefore, an interference-free analysis can be expected for the determination of amikacin in urine samples.

Besides, the selectivity of prepared MIP-based probe was studied against some similar compounds with amikacin (listed in Fig. 8). As can be seen from Fig. 8, the presence of even 10 μg mL^{-1} of examined compounds caused no considerable quenching response in the fluorescence intensity. So, a great selectivity was demonstrated for the presented sensor toward the amikacin, which is related to the specific MIP sites on the surface of g-C_3N_4 QDs. The NIP-capped g-C_3N_4 QDs showed an almost sensible response for all of tests.

Table 2
Determination of amikacin in spiked real samples by developed method.

Sample	Added (ng mL^{-1})	Found[a] (ng mL^{-1})	Recovery % ± RSD	*t*-Statistic[b]
River water	0	ND	–	–
	1.0	1.01 ± 0.04	101.03 ± 3.86	0.46
	2.0	1.96 ± 0.03	97.82 ± 1.51	2.58
Urine 1	0	ND[c]	–	–
	1.0	0.98 ± 0.02	97.60 ± 1.95	2.18
	2.0	2.03 ± 0.06	101.51 ± 3.08	0.83
Urine 2	0	ND	–	–
	1.0	0.97 ± 0.02	97.13 ± 1.77	2.88
	2.0	1.96 ± 0.03	98.05 ± 1.61	2.14

[a] Mean of three determinations ± standard deviation.
[b] *t*-Critical = 4.3 for n = 2 and P = 0.05.
[c] Not determined.

3.2.4. Application for real samples

The reliability of developed probe for amikacin was assessed by its application for the analysis of some spiked water samples (Aji-chay river water (Tabriz, Iran), and human urines (from two healthy individual) (Table 2). The recovery values were in the acceptable range (96.3–102.5%) indicating the good accuracy of our method.

4. Conclusions

High fluorescent g-C_3N_4 QDs coated with polymeric MIP layer were acceptably synthesized using the co-polymerization process of APTES and TEOS in the presence of g-C_3N_4 QDs as a proper support and amikacin as template. The characterization methods illustrated the success of this synthesis procedure. The existence of amikacin molecules during the imprinting process led to its entrapping into the produced polymeric matrix. After the washing process, specific recipient sites were generated for amikacin. On the other hand, adsorbing the amikacin into the formed MIP cavities near the g-C_3N_4 QDs decreased their fluorescence emission intensity. We applied this plan for the selective detection of amikacin in water and urine samples. The method was able to detect the amikacin concentrations as low as 3 ng mL^{-1}, without any interfering effect from similar compounds.

Acknowledgments

We thank from Baqiyatallah University of Medical Sciences and University of Tabriz for their supports.

References

[1] M.L. Yola, N. Atar, T. Eren, Determination of amikacin in human plasma by molecular imprinted SPR nanosensor, Sensors Actuators B Chem. 198 (2014) 70–76.
[2] F. Farouk, H.M. Azzazy, W.M. Niessen, Challenges in the determination of aminoglycoside antibiotics, a review, Anal. Chim. Acta 890 (2015) 21–43.
[3] Y.-F. Hu, G.-K. Li, Z.-J. Zhang, A novel luminol-based chemiluminescence method for the determination of amikacin sulfate in serum by using trivalent copper-periodate complex, J. Pharm. Anal. 3 (5) (2013) 360–366.
[4] J.M. Serrano, M. Silva, Rapid and sensitive determination of aminoglycoside antibiotics in water samples using a strong cation-exchange chromatography non-derivatisation method with chemiluminescence detection, J. Chromatogr. A 1117 (2) (2006) 176–183.
[5] C. Ezquer-Garin, L. Escuder-Gilabert, Y. Martín-Biosca, R.F. Lisart, S. Sagrado, M. Medina-Hernández, Fit-for-purpose chromatographic method for the determination of amikacin in human plasma for the dosage control of patients, Talanta 150 (2016) 510–515.
[6] A. Soliven, I.A.H. Ahmad, J. Tam, N. Kadrichu, P. Challoner, R. Markovich, A. Blasko, A simplified guide for charged aerosol detection of non-chromophoric compounds—analytical method development and validation for the HPLC assay of aerosol particle size distribution for amikacin, J. Pharm. Biomed. Anal. 143 (2017) 68–76.
[7] C.-Z. Yu, Y.-Z. He, G.-N. Fu, H.-Y. Xie, W.-E. Gan, Determination of kanamycin A, amikacin and tobramycin residues in milk by capillary zone electrophoresis with post-column derivatization and laser-induced fluorescence detection, J. Chromatogr. B 877 (3) (2009) 333–338.
[8] M.A. Omar, H.M. Ahmed, M.A. Hammad, S.M. Derayea, Validated spectrofluorimetric method for determination of selected aminoglycosides, Spectrochim. Acta A 135 (2015) 472–478.
[9] M.A. Omar, M.A. Hammad, D.M. Nagy, A.A. Aly, Development of spectrofluorimetric method for determination of certain aminoglycoside drugs in dosage forms and human plasma through condensation with ninhydrin and phenyl acetaldehyde, Spectrochim. Acta A 136 (2015) 1760–1766.
[10] M.R. Ganjali, A. Sepehri, A. Daftari, P. Norouzi, H. Pirelahi, A. Moradzadegan, Determination of salbutamol, amikacin and paromomycin sulfate by a novel sulfate

polymeric membrane sensor based on 2,6-diphenyl 4-(4-methoxyphenyl) pyrylium perchlorate, Microchim. Acta 149 (2005) 245–249.
[11] M. Rahimi-Nasrabadi, S.M. Pourmortazavi, M. Aghazadeh, M.R. Ganjali, M. Sadeghpour Karimi, P. Novrouzi, Samarium carbonate and samarium oxide; synthesis, characterization and evaluation of the photo-catalytic behavior, J. Mater. Sci. Mater. Electron. 28 (2017) 5574–5583.
[12] A. Sobhani-Nasab, S. Pourmasoud, F. Ahmadi, M. Wysokowski, T. Jesionowski, H. Ehrlich, M. Rahimi-Nasrabadi, Synthesis and characterization of $MnWO_4$/$TmVO_4$ ternary nano-hybrids by an ultrasonic method for enhanced photocatalytic activity in the degradation of organic dyes, Mater. Lett. 238 (2019) 159–162.
[13] M. Rahimi-Nasrabadi, M. Behpour, A. Sobhani-Nasab, S.M. Hosseinpour-Mashkani, $ZnFe_{2-x}La_xO_4$ nanostructure: synthesis, characterization, and its magnetic properties, J. Mater. Sci. Mater. Electron. 26 (2015) 9776–9781.
[14] M. Rahimi-Nasrabadi, M. Behpour, A. Sobhani-Nasab, M. Rangraz Jeddy, Nanocrystalline Ce-doped copper ferrite: synthesis, characterization, and its photocatalyst application, J. Mater. Sci. Mater. Electron. 27 (2016) 11691–11697.
[15] A. Sobhani-Nasab, H.R. Naderi, M. Rahimi-Nasrabadi, M.R. Ganjali, Evaluation of supercapacitive behavior of samarium tungstate nanoparticles synthesized via sonochemical method, J. Mater. Sci. Mater. Electron. 28 (2017) 8588–8595.
[16] H.R. Naderi, A. Sobhani-Nasab, M. Rahimi-Nasrabadi, M.R. Ganjali, Decoration of nitrogen-doped reduced graphene oxide with cobalt tungstate nanoparticles for use in high-performance supercapacitors, Appl. Surf. Sci. 423 (2017) 1025–1034.
[17] M. Aghazadeh, A.A.M. Barmi, H.M. Shiri, S. Sedaghat, Cathodic electrodeposition of $Y(OH)_3$ and Y_2O_3 nanostructures from chloride bath. Part II: effect of the bath temperature on the crystal structure, composition and morphology, Ceram. Int. 39 (2014) 1045–1055.
[18] M. Aghazadeh, A.A.M. Barmi, M. Hosseinifard, Nanoparticulates $Zr(OH)_4$ and ZrO_2 prepared by low-temperature cathodic electrodeposition, Mater. Lett. 73 (2012) 28–31.
[19] M. Eghbali-Arani, A. Sobhani-Nasab, M. Rahimi-Nasrabadi, S. Pourmasoud, Green synthesis and characterization of $SmVO_4$ nanoparticles in the presence of carbohydrates as capping agents with investigation of visible-light photocatalytic properties, J. Electron. Mater. 47 (2018) 3757–3769.
[20] M. Rahimi-Nasrabadi, A. Khoshroo, M. Mazloum-Ardakani, Electrochemical determination of diazepam in real samples based on fullerene-functionalized carbon nanotubes/ionic liquid nanocomposite, Sensors Actuators B Chem. 240 (2017) 125–131.
[21] J. Amani, A. Khoshroo, M. Rahimi-Nasrabadi, Electrochemical immunosensor for the breast cancer marker CA 15–3 based on the catalytic activity of a CuS/reduced graphene oxide nanocomposite towards the electrooxidation of catechol, Microchim. Acta 185 (2018) 79.
[22] A. Khoshroo, L. Hosseinzadeh, A. Sobhani-Nasab, M. Rahimi-Nasrabadi, H. Ehrlich, Development of electrochemical sensor for sensitive determination of oxazepam based on silver-platinum core–shell nanoparticles supported on graphene, J. Electroanal. Chem. 823 (2018) 61–66.
[23] J. Amani, M. Maleki, A. Khoshroo, A. Sobhani-Nasab, M. Rahimi-Nasrabadi, An electrochemical immunosensor based on poly p-phenylenediamine and graphene nanocomposite for detection of neuron-specific enolase via electrochemically amplified detection, Anal. Biochem. 548 (2018) 53–59.
[24] M. Rahimi-Nasrabadi, F. Mizani, M. Hosseini, A.H. Keihan, M.R. Ganjali, Detection of hydrogen peroxide and glucose by using $Tb_2(MoO_4)_3$ nanoplates as peroxidase mimics, Spectrochim. Acta A 186 (2017) 82–88.
[25] B. Maddah, J. Shamsi, M.J. Barsang, M. Rahimi-Nasrabadi, The chemiluminescence determination of 2-chloroethyl ethyl sulfide using luminol–$AgNO_3$–silver nanoparticles system, Spectrochim. Acta A 142 (2015) 220–225.
[26] Y.S. Borghei, M. Hosseini, M.R. Ganjali, S. Hosseinkhani, A novel BRCA1 gene deletion detection in human breast carcinoma MCF-7 cells through FRET between quantum dots and silver nanoclusters, J. Pharm. Biomed. Anal. 152 (2018) 81–88.
[27] M. Hosseini, M.R. Ganjali, Z. Vaezi, B. Arabsorkhi, M. Dadmehr, F. Faridbod, P. Norouzi, Selective recognition histidine and tryptophan by enhanced chemiluminescence ZnSe quantum dots, Sensors Actuators B Chem. 210 (2015) 349–354.
[28] S.Y. Lim, W. Shen, Z. Gao, Carbon quantum dots and their applications, Chem. Soc. Rev. 44 (1) (2015) 362–381.
[29] H.A. Kermani, M. Hosseini, M. Dadmehr, S. Hosseinkhani, M.R. Ganjali, DNA methyltransferase activity detection based on graphene quantum dots using fluorescence and fluorescence anisotropy, Sensors Actuators B Chem. 241 (2017) 217–223.
[30] Y. Wang, A. Hu, Carbon quantum dots: synthesis, properties and applications, J. Mater. Chem. C 2 (34) (2014) 6921–6939.
[31] M. Hosseini, H. Khabbaz, A.S. Dezfoli, M.R. Ganjali, M. Dadmehr, Selective recognition of glutamate based on fluorescence enhancement of graphene quantum dot, Spectrochim. Acta A 136 (2015) 1962–1966.
[32] Y. Zhan, Z. Liu, Q. Liu, D. Huang, Y. Wei, Y. Hu, X. Lian, C. Hu, A facile and one-pot synthesis of fluorescent graphitic carbon nitride quantum dots for bio-imaging applications, New J. Chem. 41 (10) (2017) 3930–3938.
[33] G. Dong, Y. Zhang, Q. Pan, J. Qiu, A fantastic graphitic carbon nitride (g-C_3N_4) material: electronic structure, photocatalytic and photoelectronic properties, J. Photochem. Photobiol. C 20 (2014) 33–50.
[34] X. Zhang, H. Wang, H. Wang, Q. Zhang, J. Xie, Y. Tian, J. Wang, Y. Xie, Single-layered graphitic-C_3N_4 quantum dots for two-photon fluorescence imaging of cellular nucleus, Adv. Mater. 26 (26) (2014) 4438–4443.
[35] X. Zhang, X. Xie, H. Wang, J. Zhang, B. Pan, Y. Xie, Enhanced photoresponsive ultrathin graphitic-phase C_3N_4 nanosheets for bioimaging, J. Am. Chem. Soc. 135 (1) (2012) 18–21.
[36] X.-L. Zhang, C. Zheng, S.-S. Guo, J. Li, H.-H. Yang, G. Chen, Turn-on fluorescence sensor for intracellular imaging of glutathione using g-C_3N_4 nanosheet–MnO_2 sandwich nanocomposite, Anal. Chem. 86 (7) (2014) 3426–3434.
[37] L. Chen, S. Xu, J. Li, Recent advances in molecular imprinting technology: current status, challenges and highlighted applications, Chem. Soc. Rev. 40 (5) (2011) 2922–2942.
[38] F. Ahmadi, J. Ahmadi, M. Rahimi-Nasrabadi, Computational approaches to design a molecular imprinted polymer for high selective extraction of 3,4-methylenedioxymethamphetamine from plasma, J. Chromatogr. A 1218 (2011) 7739–7747.
[39] A. Hillberg, K. Brain, C. Allender, Molecular imprinted polymer sensors: implications for therapeutics, Adv. Drug Deliv. Rev. 57 (12) (2005) 1875–1889.
[40] J. Wackerlig, R. Schirhagl, Applications of molecularly imprinted polymer nanoparticles and their advances toward industrial use: a review, Anal. Chem. 88 (1) (2015) 250–261.
[41] M. Mehrzad-Samarin, F. Faridbod, M.R. Ganjali, A luminescence nanosensor for Ornidazole detection using graphene quantum dots entrapped in silica molecular imprinted polymer, Spectrochim. Acta A 206 (2019) 430–436.
[42] T. Alizadeh, M. Akhoundian, M.R. Ganjali, An innovative method for synthesis of imprinted polymer nanomaterial holding thiamine (vitamin B1) selective sites and its application for thiamine determination in food samples, J. Chromatogr. B 1084 (2018) 166–174.
[43] M. Akhoundian, T. Alizadeh, M.R. Ganjali, F. Rafiei, A new carbon paste electrode modified with MWCNTs and nano-structured molecularly imprinted polymer for ultratrace determination of trimipramine: the crucial effect of electrode components mixing on its performance, Biosens. Bioelectron. 111 (2018) 27–33.
[44] Y. Ma, S. Xu, S. Wang, L. Wang, Luminescent molecularly-imprinted polymer nanocomposites for sensitive detection, TrAC Trends Anal. Chem. 67 (2015) 209–216.
[45] M. Panagiotopoulou, Y. Salinas, S. Beyazit, S. Kunath, L. Duma, E. Prost, A.G. Mayes, M. Resmini, B. Tse Sum Bui, K. Haupt, Molecularly imprinted polymer coated quantum dots for multiplexed cell targeting and imaging, Angew. Chem. Int. Ed. 55 (29) (2016) 8244–8248.